DIRECT RHO-ASSOCIATED KINASE INHIBITON INDUCES COFILIN DEPHOSPHORYLATION AND NEURITE OUTGROWTH IN PC-12 CELLS

ZHIQUN ZHANG[1,2,3], ANDREW K. OTTENS[1,2,3], STEPHEN F. LARNER[2,3], FIRAS H. KOBEISSY[1,2,3], MELISSA L WILLIAMS[3], RONALD L. HAYES[2,3,4] and KEVIN K. W. WANG[1,2,3,4]*
[1]Centers for Neuroproteomics and Biomarkers Research and [2]Traumatic Brain Injury Studies, [3]Departments of Neuroscience and [4]Psychiatry, McKnight Brain Institute, P.O. Box 100256, University of Florida, 100 S. Newell Drive, Gainesville, Florida 32610, USA

Abstract: Axons fail to regenerate in the adult central nervous system (CNS) following injury. Developing strategies to promote axonal regeneration is therapeutically attractive for various CNS pathologies such as traumatic brain injury, stroke and Alzheimer's disease. Because the RhoA pathway is involved in neurite outgrowth, Rho-associated kinases (ROCKs), downstream effectors of GTP-bound Rho, are potentially important targets for axonal repair strategies in CNS injuries. We investigated the effects and downstream mechanisms of ROCK inhibition in promoting neurite outgrowth in a PC-12 cell model. Robust neurite outgrowth (NOG) was induced by ROCK inhibitors Y-27632 and H-1152 in a time- and dose-dependent manner. Dramatic cytoskeletal

* Corresponding author; e-mail: kwang@psychiatry.ufl.edu, tel: 352-392-3681, fax: 352-392-2579

reorganization was noticed upon ROCK inhibition. NOG initiated within 5 to 30 minutes followed by neurite extension between 6 and 10 hours. Neurite processes were then sustained for over 24 hours. Rapid cofilin dephosphorylation was observed within 5 minutes of Y-27632 and H-1152 treatment. Re-phosphorylation was observed by 6 hours after Y-27632 treatment, while H-1152 treatment produced sustained cofilin dephosphorylation for over 24 hours. The results suggest that ROCK-mediated dephosphorylation of cofilin plays a role in the initiation of NOG in PC-12 cells.

Key words: Neurite outgrowth, ROCK, Y-27632, PC-12, Cofilin, Actin dynamics

INTRODUCTION

Unlike axons in the peripheral nervous system, in the adult central nervous system (CNS) axons fail to regenerate spontaneously. The lack of regeneration is due to a diverse class of neuritogenic inhibitors that prevail in the CNS. Some of these inhibitors have already been identified, such as Nogo-A, myelin associated glycoprotein (MAG) [1], chondroitin sulfate proteoglycans (CSPGs) and oligodendrocyte myelin glycoprotein (OMgp) [2, 3]. Previous studies showed that by overcoming the inhibitory effects of Nogo-A, CSPG, and MAG through inhibition of small Rho-GTPases and Rho kinase can promote axonal regeneration [4-7]. The mature CNS also contains neurotrophic factors that promote growth and survival of neurons. The best studied is nerve growth factor (NGF) [8]; however, several other molecules exhibit neurotrophic properties, including fibroblast growth factor (FGF), brain-derived neurotrophic factor (BDNF) and neurotrophin-3 (NT-3) [9, 10]. Interestingly, NGF and NT-3 promote axonal outgrowth via the suppression of Rho-A activity [11, 12]. Thus, there is accumulating evidence linking Rho and associated Rho kinases with permissive as well as inhibitory pathways of neurite outgrowth. Strategies for promoting axonal regeneration in the CNS are therapeutically attractive for treatment of various diseases such as traumatic brain injury, stroke and Alzheimer's disease.

ROCKs (also known as Rho kinases), a class of serine/threonine kinases, were the first downstream effectors of Rho to be discovered [13]. Numerous studies showed that ROCKs mediate a large proportion of the signals from Rho in regulating cytoskeleton reorganization [14, 15]. Initially, activation of ROCKs was characterized by direct phosphorylation of myosin light chain (MLC) [16] and by indirect inhibition of MLC phosphatase (MLCP) [17] in mediating Rho-A induced stress fibers and focal adhesions. ROCKs consist of an amino-terminal kinase domain and an autoinhibitory carboxy-terminal region, which includes the Rho-binding (RB) domain and the pleckstrin homology (PH) domain. Both the RB and PH domains can independently interact with the amino-terminal kinase domain to inactivate the enzyme. Conversely, Rho

interacts with the RB domain to disrupt the negative regulation between the kinase domain and the autoinhibitory region, thereby freeing kinase activity. So far, two ROCK isoforms have been identified: ROCK I (also known as ROKβ and P160ROCK) and ROCK II (ROKα). The kinase domains of ROCK I and ROCK II are 92% identical, and so far there is no evidence that they perform different functions [18]. Recently, the Rho-ROCK pathway was demonstrated to mediate neurite retraction, growth cone collapse and axonal outgrowth through ROCK inhibition of an inhibitory substrate such as MAG in dorsal root ganglions (DRG) [4, 14].

The rat pheochromocytoma cell line, PC-12, has been widely used as an important model for neuronal differentiation. PC-12 cells differentiate into a neuronal phenotype in response to various neurotrophins. For instance, nerve growth factor (NGF) treated PC-12 cells exhibit proliferation arrest, neurite outgrowth (NOG) and electrical excitability [19]. In previous studies we also demonstrated that repeated amphetamine treatment induces NOG in PC-12 cells, similar to that found with known neurotrophic factors [20]. Moreover, PC-12 cells elicit NOG via Rho inhibition by *Clostridium b.* C-3 exoenzyme treatment [5, 21], making it an invaluable model system for studying potential Rho-ROCK downstream signal transduction pathways in NOG.

Cytoskeletal reorganization through actin and microtubule remodeling plays a striking role in NOG. Thus, it is essential to understand the signaling pathways that control cytoskeleton dynamics [22]. Rho GTPase has been shown to influence actin cytoskeleton dynamics [21, 23]. ROCKs also mediate signals to the actin cytoskeleton through various substrates, such as adducin and LIM kinase (LIMK) [23]. In turn, LIMK phosphorylates cofilin, an actin associated protein, which binds to actin and serves to enhance depolymerization of actin filaments. Once phosphorylated, cofilin is inactivated and loses its filament severing and monomer binding abilities [24, 25]. In addition, ROCKs phosphorylate other neurite intermediate filament or microtubule-associated proteins such as NF-L [26], Tau and MAP2 [27].

A number of ROCK inhibitor compounds have been developed, including H-89, HA-1077, Y-27632 [28], H-1152 [29] and Wf-536 [30]. Among commercially available inhibitors, (R)-(+)-*trans*-N-(4-Pyridyl)-4-(1-aminoethyl)-cyclohexane-carboxamide (Y-27632), has shown high potency and selectivity for ROCK inhibition [14, 31]. This selective inhibition of ROCKs makes Y-27632 very useful for evaluating ROCK functions in CNS since ROCKs are highly expressed in the brain. In this study, the role of ROCK inhibitor (Y-27632 or H-1152) was systematically evaluated for promoting NOG in the well-defined PC-12 model. Dynamics in cell morphology and cytoskeleton components (actin, cofilin and βIII-tubulin) were characterized following treatment with the ROCK inhibitor Y-27632. Results suggest ROCK inhibition might be a potential therapeutic avenue for promoting NOG after CNS injury.

MATERIALS AND METHODS

Chemicals and antibodies
Culture media and sera were obtained from Gibco Inc. (Rockville, MD). Y-27632, H-1152, Ro-32-0432, PD 98059, and H-89 were purchased from Calbiochem (San Diego, CA). The primary antibodies used include: polyclonal anti- phospho-cofilin and cofilin (Cell Signaling, Beverly, MA), monoclonal anti-βIII-tubulin (Covance, Denver, PA) and FITC-conjugated phalloidin (Molecular Probes, Eugene, OR).

Cell culture
PC-12 cells were maintained at 37ºC in Dulbeco's modified Eagle's medium (DMEM) supplied with 10% fetal bovine serum (FBS), 5% heat-inactivated horse serum, 100 μg/mL of streptomycin, 100 U/mL of penicillin and 1% Fungizone (Gibco, Rockville, MD) in a humidified 5% CO_2 incubator. To induce neurite outgrowth, PC-12 cells were plated in the same medium with Y-27632 or H-1152. Each Rock inhibitor was prepared as a 25 mM stock solution in dimethlsulfoxide (DMSO) and added directly into the medium. An equal amount of DMSO was added to control plates. Micrographs of cells were taken at 32x with an Axiocam digital camera using a Zeiss Axiovert 135 microscope. For the kinase inhibition study, PC-12 cells were treated with 25 μM Y-27632 for 2 hours, and then continued to be co-treated with 300 nM RO-32-0432 or 500 nM H-89 or 30 μM PD 98059 for 14 hours.

Quantification of neurite outgrowth
Cell processes were defined as neurites when longer than the diameter of the cell body. The percentage of neurite-bearing cells was calculated as the number of cells with one or more neurites divided by the total cell number [20]. Neurite length was evaluated by manually tracing the longest neurite per cell using the software ImageJ (version 1.29, NIH, USA) and referenced to a known length. Each experiment was conducted in triplicate, and images were taken with 15 or more cells per field. For each experiment, at least 50 cells were randomly measured.

Immunoblotting
PC-12 cells were treated for various time periods, washed twice with phosphate-buffered saline (PBS), and solubilized with lysis buffer containing 20 mM Tris-HCl, pH 7.4, 150 mM NaCl, 5 mM EDTA, 5 mM EGTA, 1% Triton X-100, 1 mM NaF, 1 mM Na_3VO_4, and a protease inhibitor cocktail tablet (Roche, Indianapolis, IN). The cell lysates were briefly sonicated before clarification by centrifugation at 15,000 g for 10 minutes at 4ºC. The protein concentration of the supernatant was determined by a modified Lowry method (DC Protein Assay Kit, Bio-Rad, Hercules, CA). Samples (20 μg protein) were resolved by 10-20% sodium dodecyl sulfate-polyacrylamide gel electrophoresis (SDS-PAGE) and transferred onto a polyvinylidene difluoride (PVDF) membrane by the semi-dry

method. Membranes were blocked with 5% non-fat milk in tris-buffered saline containing 0.1% tween-20 (TBST) and then incubated with the primary antibody in 5% non-fat milk in TBST at 4ºC overnight. Following a series of washes with TBST, membranes were incubated for one hour at room temperature with a biotinylated secondary antibody. Following another series of washes, the membrane was incubated with avidin-conjugated alkaline phosphatase for 30 minutes. Proteins were visualized using nitroblue tetrazolium and 5-bromo-4chloro-3-indolyl phosphate. The membranes were scanned, and the optical density of the bands was quantified with the software ImageJ (version 1.29x, NIH, USA).

Immunocytochemistry
PC-12 cells were seeded onto LabTek II chamber slides (Nunc, Naperville, IL) followed by overnight incubation. On the next day, the medium was replaced with or without 25 μM Y-27632. Twenty-four hours following treatment, PC-12 cells were fixed with 4% paraformaldehyde (PFA) in PBS for 10 minutes, washed with PBS and permeabilized with 0.1% Triton X-100 in PBS for 5 minutes. F-actin was fluorescently labeled with 5 units/mL FITC-conjugated phalloidin for 20 minutes at room temperature. βIII-tubulin staining was performed following a one-hour blocking step in 10% goat serum at room temperature. Then the cells were incubated overnight at 4ºC with monoclonal rabbit anti-βIII-tubulin at a dilution of 1:2000. Alexa 488-conjugated goat-anti-rabbit secondary antibody (Molecular Probes, Eugene, OR) was added at a dilution of 1:1000, followed by washing with PBS. The cells were mounted using medium with 4, 6-diamidine-2-phenylindole (DAPI) (Vector Laboratories, Burlingame, CA). Fluorescence images were captured with a 20x objective on the Zeiss Axioplan 2 Fluorescence Microscope with a CCD camera and combined using SPOT imaging software (Diagnostic Instruments, Sterling Heights, MI).

RESULTS

Dose-dependent neurite outgrowth induced by ROCK inhibition in PC-12 cells
The effect of ROCK inhibitor Y-27632 on a low-density culture of PC-12 cells over multiple concentrations is shown in Figure 1. At the low dose of 0.01 μM, PC-12 cells appear similar with control cells that are slightly larger and rounder, but possess few visible neurites (Fig. 1 A, top panel). At higher Y-27632 doses, from 1 μM to 100 μM, an increased number of PC-12 cells presented multiple long-branched neurites in a dose dependent fashion, compared to sparse growth in controls (Fig. 1 B-F, top panel). The percentage of neurite-bearing cells peaked at 90% between 25 and 100 μM (Fig. 1, bottom panel). However, at 100 μM, cell detachment from the substrate and neurite loss was noticed after 48 hours of exposure (data not shown).
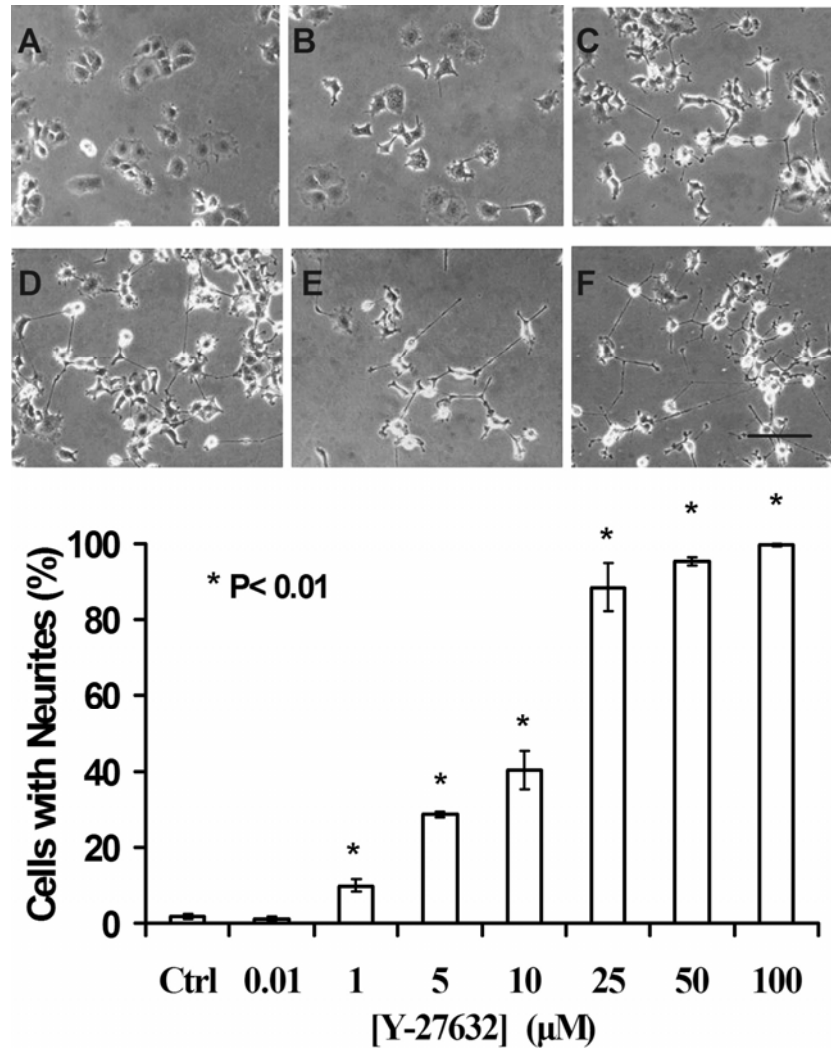
Fig. 1. Neurite outgrowth of PC-12 cells in response to ROCK inhibitor Y-27632 in a dose-dependent manner. *Top panel*: A through F are phase-contrast images of PC-12 cells following treatment by different concentration of Y-27632 for 24 hours. (A) 0.01 μM; (B) 1 μM; (C) 5 μM; (D) 10 μM; (E) 25 μM; and (F) 100 μM of Y-27632. Scale bar represents 50 μm. *Bottom Panel*: Quantification of neurite outgrowth following Y-27632 treatment for 24 hours. Cells with at least one neurite greater than the diameter of the cell body were counted and expressed as a percentage of the total number of cells in a field. For each experiment, at least 50 cells were randomly measured. Data shown are mean values ± S.E.M, n = 3. Statistical significance of differences ($P < 0.01$) between the control and each treated group was determined by one-way ANOVA with Dunnett's multiple comparison tests.
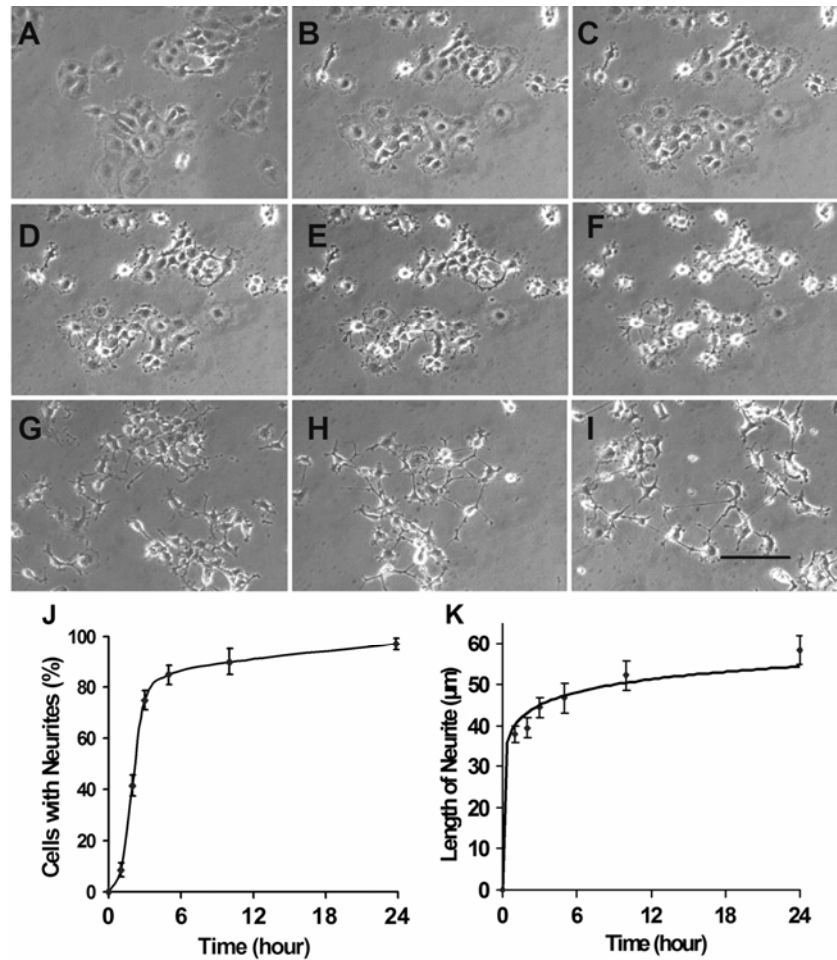
Fig. 2. ROCK inhibitor Y-27632 induced neurite outgrowth in PC-12 cells in a time-dependent manner. Panels A through I are phase-contrast images of PC-12 cells following 25 μM Y-27632 treatment for different time points: (A) Control (B) 5 min; (C) 10 min; (D) 30 min; (E) 1 hr; (F) 3 hr; (G) 6 hr; (H) 10 hr; and (I) 24 hr. Arrows indicate examples of typical neurite outgrowth in PC-12 cells over time. Cells were plated onto 6-well plates at a cell density of 4 x 10^3/cm^2. Scale bar represents 50 μm. Quantification of neurite outgrowth post Y-27632 treatment in PC-12 cells. Quantification of cells with neurites (J) and neurite lengths (K) were performed after PC-12 cells were treated with 25 μM Y-27632 at various time points. The length of the longest neurite was counted for cells with at least one identified neurite. Neurite length was determined by manually tracing the length of the longest neurite per cell. For each experiment, at least 50 cells were randomly measured. Values represent means ± S.E.M. n = 4.
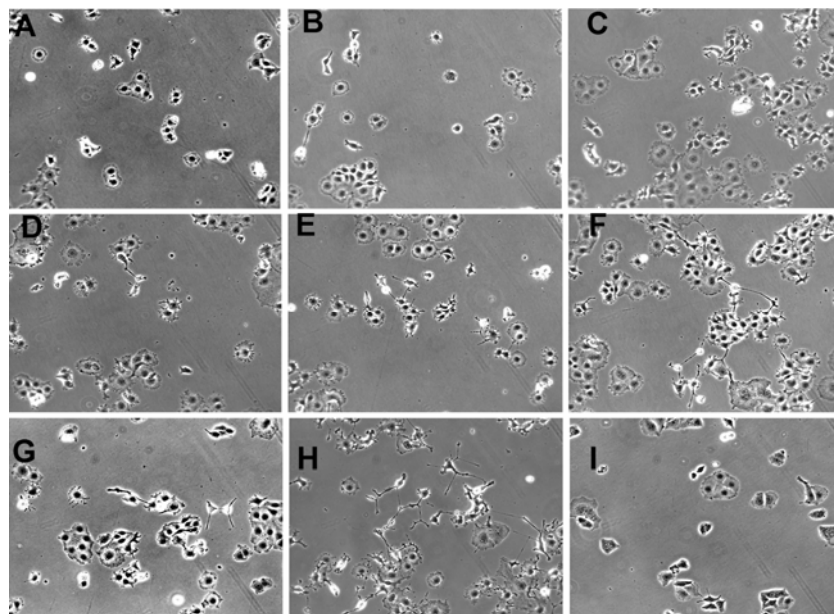
Fig. 3. ROCK inhibitor H-1152 induced neurite outgrowth in PC-12 cells in a time- and concentration-dependent manner. Panels A through F are phase-contrast images of PC-12 cells following 1 μM H-1152 treatment for different time points: (A) 5 min; (B) 30 mins; (C) 2 hr; (D) 6 hr; (E) 12 hr; (F) 24 hr; or with 0.1 μM H-1152 for 24 hr (G), 10 μM H-1152 for 24 hr (H) or no comound for 24 hr (I).

Dynamics of neurite outgrowth in ROCK inhibitor treated PC-12 cells

To further examine NOG dynamics after ROCK inhibition, we executed a time course analysis of NOG in PC-12 cells using 25 μM Y-27632. NOG initiated within 5 minutes with visible small protrusion veils (lamellipodia) (Fig. 2B), followed by a f ew spikes (filopodia) 10 minutes later (Fig. 2C). Prominent neurite elongation was observed between 30 minutes and 6 hours, while fully extended neurites appeared following 6 to 10 hours of treatment, which were sustained for 24 hours after Y-27632 stimulation (Fig. 2D-I). The number of neurite-bearing cells also rapidly increased after Y-27632 exposure, with greater than 85% of the cells having neurites within 6 hours (Fig. 2J), Neurite extension was biphasic, with a rapid increase within 6 hours followed by a more gradual extension to maximal length by 24 hours (Fig. 2K). Since protein kinase inhibitory agents, including Y-27632, can cross-inhibit other protein kinases, we tested the more specific ROCK inhibitor H-1152 (Fig. 3). We observed that even at the low concentration of 1 μM, H-1152 produced a rapid cell shape change, with lamellipodia and filopodia developing within 5-30 minutes (Fig. 3B, C), and fully extended neurites formed by 24 hours (Fig. 3F). The same NOG effect was observed with a 10 μM treatment of H-1152 (Fig. 3H), while 0.1 μM produced only a partial NOG within 24 hours (Fig. 3G).

Remodeling of cytoskeletal architecture in ROCK inhibition mediated neurite outgrowth

The cytoskeleton is considered a principal determinant of NOG, so we examined cytoskeleton reorganization during Y-27632 treatment [22]. FITC-phalloidin F-actin immunostaining and neuronal specific βIII-tubulin immunostaining (green) were performed against DAPI staining (blue) of the nuclear DNA, respectively. Before treatment, PC-12 cells were round and F-actin was uniformly localized in the periphery of the soma (triangle in Fig. 4A), and βIII-tubulin was evenly distributed within the cell body (Fig. 4C). After 12 hours treatment, F-actin accumulated in growth cone-like structures (short arrow in Fig. 4B), newly formed neurites (long arrow in Fig. 4B) and lamellipodia (triangle in Fig. 4B). In comparison, βIII-tubulin was preferentially concentrated along the nascent neurites (arrow in the Fig. 4D).
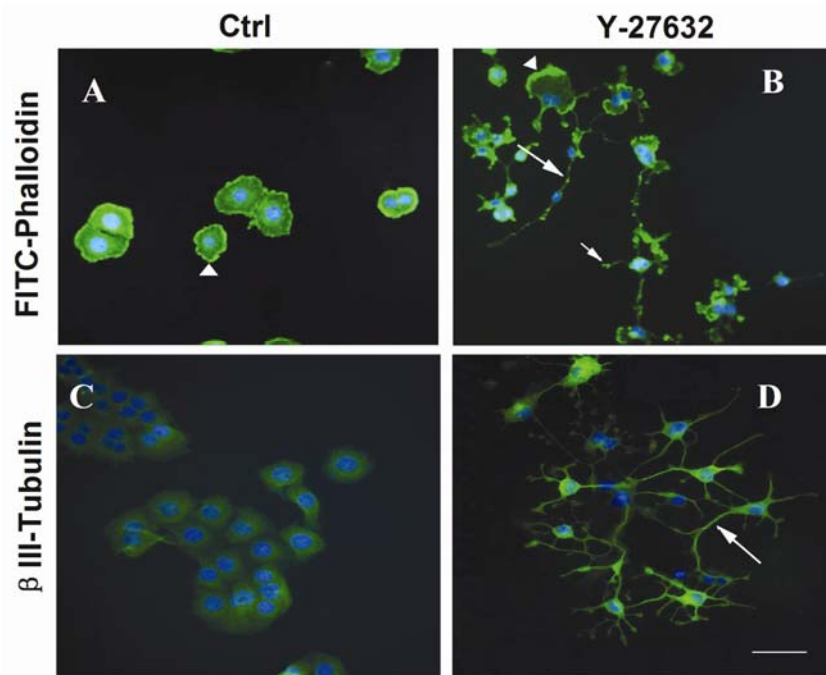

Fig. 4. Reorganization of cytoskeletal architecture in ROCK inhibition mediated neurite outgrowth. PC-12 cell nuclei were visualized with DAPI-DNA staining (blue). Panel A and B were FITC-phalloidin F-actin-staining (green) following treatment with Y-27632. Before treatment, F-actin is uniformly localized in the periphery of the soma (triangle in panel A). After 12-hour treatment, F-actin became highly accumulated in growth cone-like structures (short arrow in panel B), the neurites (long arrow in panel B) and lamellipodia (triangle in panel B). Panels C through D were Alexa 488-conjugated neuronal specific βIII-tubulin immunostaining (green). Most βIII-tubulin is concentrated in nascent neurites (arrow in panel D). Cells were treated by DMSO as a control (A, C) or 25 μM Y-27632 (B, D) for 12 hours prior to fixation. Scale bar represents 50 μm.

ROCK inhibition induces transient cofilin dephosphorylatlion
The polymerization/depolymerization of actin was shown to be necessary for NOG [23]; thus, we investigated the signaling pathways involved in actin dynamics. Cofilin is the most well characterized stimulus-responsive mediator of actin dynamics. Cofilin dissociates from F-actin when phosphorylated by LIMK. Since LIMK is a direct downstream effector of ROCK, ROCK inhibition decreases LIMK1 activity and dephosphorylates cofilin. In a series of experiments, we sought to identify the cytoskeleton signal transduction pathways through which Y-27632 mediated NOG in PC-12 cells. The morphology change of PC-12 cells in response to Y-27632 indicated that the
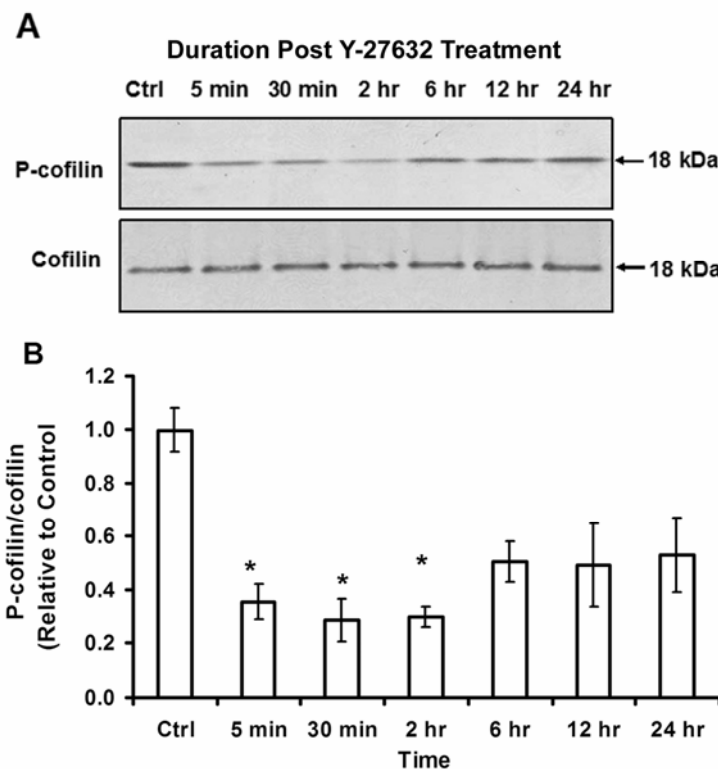

Fig. 5. Immunoblot analysis of cofilin phosphorylation following Y-27632 treatment. A - PC-12 cells were treated with ROCK inhibitor (Y-27632; 25 μM) for various time points. Total protein lysate were extracted for immunoblotting analysis with phospho-cofilin (P-cofilin) and total cofilin antibodies. Representative blots were shown here. B - Densitometric analyses of cofilin immunoblots were performed. The optical densities of phospho-cofilin were normalized to the corresponding values for total cofilin. Values represent means ± S.E.M. n = 4. Statistical significance of differences between the control and each treated group was determined by one-way ANOVA with Dunnett's multiple comparison tests. A difference was considered to be statistically significant when the P value was less than 0.01 (*$P < 0.01$).

initiation of NOG occurred within 5 minutes. Correlated with the morphological change, more than 60% of cofilin underwent dephosphorylation within 5 minutes. Subsequent partial recovery of phospho-cofilin was noticed during the neurite elongation and maintenance periods (6 to 24 hr) (Fig. 5A and B). There was no change in the total expression level of cofilin during ROCK inhibitor treatment (Fig. 5A). Thus, dephosphorylation-phosphorylation of cofilin appears to be involved in the initiation of NOG.
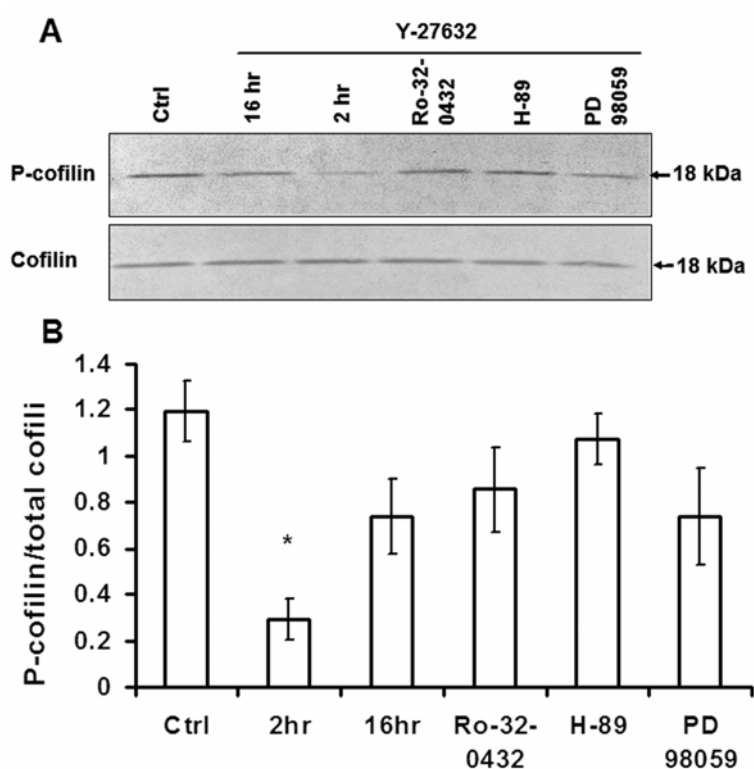

Fig. 6. Effect of various protein kinase inhibitiors on cofilin rephosphorylation in the presence of Y-27632. A - PC-12 cells were treated with ROCK inhibitor (Y-27632; 25 μM) for 2 h. For the same conditions, protein kinase-A (H-89; 500 nM), protein kinase-C (Ro-32-0432, 300 nM) or MAPK (PD98059, 30 μM) attenuated cofilin rephosphoryaltion. The cells were further incubated to 16 hour before cell lysate was collected for immunoblotting analysis with phospho-cofilin (P-cofilin) and total cofilin antibodies. B - Densitometric analyses of cofilin immunoblots were performed. The optical densities of phospho-cofilin were normalized to the corresponding values for total cofilin. Values represent average from three experiments (*P < 0.01).
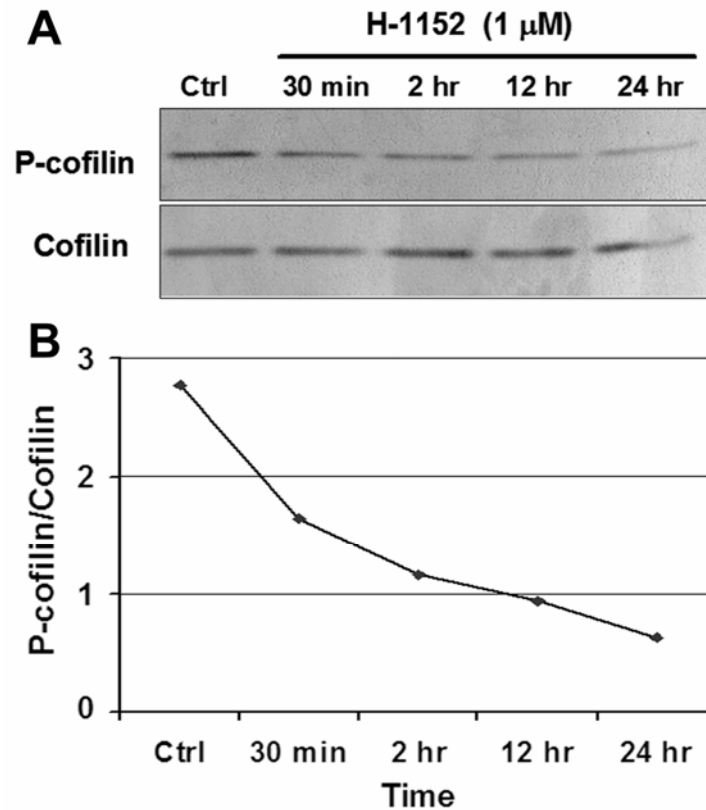
Fig. 7. Persistent cofilin phosphorylation following ROCK inhibitor H-1152 treatment. A - PC-12 cells were treated with ROCK inhibitor (H-1152; 1 μM) for various time points (30 min, 2 h, 12 h and 24 h). Total protein lysate were extracted for immnuoblotting analysis with phosphor-cofilin (P-cofilin) and total cofilin antibodies. Representative blots were shown here. B - Densitometric analyses of cofilin immunoblots were performed. The optical densities of P-cofilin were normalized to the corresponding values for total cofilin. Values represent means from two separate experiments.

We were intrigued by the observation that cofilin underwent partial re-phosphorylation following the initial phase of dephosphorylation, despite the presence of a constant level of ROCK inhibitor (Y-27632, 25 μM) (Fig. 5). We hypothesized that this involved additional protein kinases or protein kinase cross talk. Protein kinase-A, protein kinase C and MAPK have all been implicated in neurite outgrowth in PC-12 cells [32-34]. PC-12 cells were first subjected to 25 μM of Y-27632 for the maximal cofilin dephosphorylation. Then various protein kinase inhibitors were introduced to see if they would suppress cofilin re-phosphorylation. However, attenuated re-phosphorylation was not observed with any of the kinase inhibitors (Fig. 6). To further confirm that cofilin

dephosphorylation is ROCK mediated, we again employed a second specific ROCK inhibitor H-1152 (Fig. 7). A rapid dephosphorylation of cofilin was observed at a low concentration of H-1152 (1 μM) within 30 minutes. Interestingly, H-1152 differed from Y-27632 in that the level of dephosphorylated cofilin was sustained for up to 24 hours (Fig. 7).

DISCUSSION

Although induction of NOG in PC-12 cells by ROCK inhibition has been reported in previous studies [35-37], this is the first comprehensive biochemical analysis of this important phenomenon. Birkenfeld *et al.* [35] only briefly described the effects of Y-27632 on NOG using the less selective ROCK inhibitor Y-27632. For the first time, we report complimentary data using the more specific H-1152 inhibitor (Fig. 1-3). Both Y-27632 and H-1152 rapidly initiated NOG within 5 to 30 minutes with the formation of small protrusions (neurite initiation) followed by neurite extension in 6 to 10 hours (elongation) (Fig. 2). Concurrently, both ROCK inhibitors produce rapid cofilin-dephosphorylation.

Since NGF induced NOG in PC-12 cells by activating protein kinase C (PKC) [32], it is possible that Y-27632 might exert its effects on PKC. However, this possibility was ruled out as PKC was not inhibited at 10 μM of Y-27632, yet 1-5 μM Y-27632 already produced NOG (Fig. 1). Y-27632 is also known to inhibit MAP kinase activated protein kinase-1b (MAPAP-K1b) (IC_{50} 19 μM), but at a higher concentration than ROCK (IC_{50} 800 nM) *in vitro* [31]. By observing NOG at the low 1-5 μM concentration of Y-27632 it is unlikely that the effect can be attributed to MAPAP-K1b inhibition. Furthermore, the more selective ROCK inhibitor H-1152 [29, 38] produced the same NOG effect at 1 μM (Fig. 3).

Neuronal differentiation processes were mediated by cytoskeletal reorganization, as observed with F-actin and microtubules. Two major F-actin networks were observed in the filopodia and lamellipodia of the neuronal growth cones [22]. Neuron-specific βIII-tubulin usually is expressed in cell bodies and is highly concentrated in neurites of mature neurons [39]. In our study, F-actin accumulated in growth cone-like structures, lamellipodia and neurites (Fig. 4B), whereas βIII-tubulin was preferentially enriched along the nascent neurites of PC-12 cells following ROCK inhibition (Fig. 4D). Similar to NGF-induced NOG, ROCK inhibition induced PC-12 cell differentiation into a neuronal phenotype, indicated by neuronal specific βIII-tubulin antibody staining and morphological changes (Fig. 4D). Thus, differentiated PC-12 cells are representative of neurons in this study, and were used to explore downstream ROCK pathways in NOG.

Interestingly, ROCK inhibitor induced a rapid decrease and then subsequent gradual increase in the phosphorylation of cofilin, which correlated with the initiation and elongation of neurites (Fig. 5). It is important to point out that

Maekawa *et al.* had previously established that ROCK inhibition causes cofilin dephosphorylation through LIMK-1 [24]. However, our data indicates a relationship between ROCK-cofilin dephosphorylation and neurite outgrowth. Tojima and Ito recently proposed a signal transduction cascade that involves ROCK inhibition decreasing LIMK1 activity and dephosphorylating cofilin, thus inhibiting neuritogenesis [22]. Yet, based on our studies, instead of inhibiting neuritogenesis, our results showed that cofilin dephosphorylation coincided with NOG initiation (5 to 30 minutes), while cofilin re-phosphorylation occurred during neurite elongation and maintenance phases (6 to 24 hours) (Fig. 5A). Our results were consistent with the work of Aizawa *et al*, where a sequential cofilin phosphorylation-dephophorylation cycling occured during semaphoring 3A (Sema-3A) treatment on DRG cells [40]. Sema-3A, a chemorepulsive axonal guidance molecule, induces growth cone collapse via the LIMK-cofilin pathway that regulates actin-filament dynamics.

The dynamic cofilin dephosphorylation-phosphorylation found in our work indicates that in addition to LIMK, other signaling pathways may also be involved in the mechanism of regulating cofilin cycling during NOG of PC-12 cells. Upon ROCK inhibition LIM kinases are inactivated leading to dephosphorylation of cofilin and resulting in massive new barbed ends for initiation neurites. We attempted to elucidate the mechanism of cofilin re-phosphorylation shown during longer Y-27632 treatments (6 h to 24 h) (Fig. 5). Since protein kinase A, C and MAPK have all been previously implicated in NOG of PC-12 cells [32-34], we tested the potential effects of pharmacological inhibitors of these kinases on post-Y-27632 cofilin rephosphorylation. However, protein kinase A, C and MAPK inhibition all failed to prevent cofilin re-phosphorylation (Fig. 6). Other signaling pathways, such as inhibition of the Slingshot phosphatase [41] or type 1 and type 2A serine/threonine phosphatases [42], may be involved in the re-phosphorylation of cofilin, which in turn leads to actin polymerization, and subsequently contributes to the elongation and maintenance of neurites. This mechanism may also apply to the formation and/or stability of essential actin-based structures in growth cones and postsynaptic densities [43]. In addition to inhibiting ROCKs, Y-27632 also inhibits protein kinase C-related kinase (PRK)$_2$ *in vitro*, which may contribute to the dephosphorylation-phosphorylation dynamics of cofilin [28]. We thus tested a more specific ROCK inhibitor (H-1152) [29, 38]. It is of interest to note that, when PC-12 cells were treated with H-1152, cofilin dephosphorylation was sustained for 24 hours without notable re-phosphorylation (Fig. 7). Further work is needed to understand crosstalk between signaling cascades in ROCK inhibition mediated NOG. Understanding the signaling mechanisms of ROCK inhibition mediated NOG opens up the possibility for developing novel strategies to promote axon regeneration *in vivo*. Clinically, the use of a ROCK inhibitor may be useful for developing therapies in CNS following damage by Alzheimer's disease [44], spinal cord injury [45], traumatic brain injury [46] and stroke [47].

REFERENCES

1. McKerracher, L., David, S., Jackson, D.L., Kottis, V., Dunn, R.J. and Braun, P.E. Identification of myelin-associated glycoprotein as a major myelin-derived inhibitor of neurite growth. **Neuron** 13 (1994) 805-811.
2. McKerracher, L. and David, S. Easing the brakes on spinal cord repair. **Nat. Med.** 10 (2004) 1052-1053.
3. Wang, K.C., Koprivica, V., Kim, J.A., Sivasankaran, R., Guo, Y., Neve, R.L. and He, Z. Oligodendrocyte-myelin glycoprotein is a Nogo receptor ligand that inhibits neurite outgrowth. **Nature** 417 (2002) 941-944.
4. Fournier, A.E., Takizawa, B.T. and Strittmatter, S.M. Rho kinase inhibition enhances axonal regeneration in the injured CNS. **J. Neurosci.** 23 (2003) 1416-1423.
5. Lehmann, M., Fournier, A., Selles-Navarro, I., Dergham, P., Sebok, A., Leclerc, N., Tigyi, G. and McKerracher, L. Inactivation of Rho signaling pathway promotes CNS axon regeneration. **J. Neurosci.** 19 (1999) 7537-7547.
6. Yamashita, T., Higuchi, H. and Tohyama, M. The p75 receptor transduces the signal from myelin-associated glycoprotein to Rho. **J. Cell Biol.** 157 (2002) 565-570.
7. Yamashita, T., Fujitani, M., Yamagishi, S., Hata, K. and Mimura, F. Multiple signals regulate axon regeneration through the nogo receptor complex. **Mol. Neurobiol.** 32 (2005) 105-112.
8. Bonini, S., Rasi, G., Bracci-Laudiero, M.L., Procoli, A. and Aloe, L. Nerve growth factor: neurotrophin or cytokine? **Int. Arch. Allergy Immunol.** 131 (2003) 80-84.
9. Ebadi, M., Bashir, R.M., Heidrick, M.L., Hamada, F.M., Refaey, H.E., Hamed, A., Helal, G., Baxi, M.D., Cerutis, D.R. and Lassi, N.K. Neurotrophins and their receptors in nerve injury and repair. **Neurochem. Int.** 30 (1997) 347-374.
10. Petruska, J.C. and Mendell, L.M. The many functions of nerve growth factor: multiple actions on nociceptors. **Neurosci. Lett.** 361 (2004) 168-171.
11. Ozdinler, P.H. and Erzurumlu, R.S. Regulation of neurotrophin-induced axonal responses via Rho GTPases. **J. Comp. Neurol.** 438 (2001) 377-387.
12. Yamaguchi, Y., Katoh, H., Yasui, H., Mori, K. and Negishi, M. RhoA inhibits the nerve growth factor-induced Rac1 activation through Rho-associated kinase-dependent pathway. **J. Biol. Chem.** 276 (2001) 18977-18983.
13. Kwon, B.K., Borisoff, J.F. and Tetzlaff, W. Molecular targets for therapeutic intervention after spinal cord injury. **Mol. Intervent.** 2 (2002) 244-258.

14. Amano, M., Fukata, Y. and Kaibuchi, K. Regulation and functions of Rho-associated kinase. **Exp. Cell Res.** 261 (2000) 44-51.

15. Hall, A. Rho GTPases and the control of cell behaviour. **Biochem. Soc. Trans.** 33 (2005) 891-895.

16. Somlyo, A.P. and Somlyo, A.V. Signal transduction by G-proteins, rho-kinase and protein phosphatase to smooth muscle and non-muscle myosin II. **J. Physiol.** 522 Pt 2 (2000) 177-185.

17. Kawano, Y., Fukata, Y., Oshiro, N., Amano, M., Nakamura, T., Ito, M., Matsumura, F., Inagaki, M. and Kaibuchi, K. Phosphorylation of myosin-binding subunit (MBS) of myosin phosphatase by Rho-kinase in vivo. **J. Cell Biol.** 147 (1999) 1023-1038.

18. Riento, K. and Ridley, A.J. Rocks: multifunctional kinases in cell behaviour. **Nat. Rev. Mol. Cell Biol.** 4 (2003) 446-456.

19. Greene, L.A. and Tischler, A.S. Establishment of a noradrenergic clonal line of rat adrenal pheochromocytoma cells which respond to nerve growth factor. **Proc. Natl. Acad. Sci.** 73 (1976) 2424-2428.

20. Park, Y.H., Kantor, L., Guptaroy, B., Zhang, M., Wang, K.K. and Gnegy, M.E. Repeated amphetamine treatment induces neurite outgrowth and enhanced amphetamine-stimulated dopamine release in rat pheochromocytoma cells (PC12 cells) via a protein kinase C- and mitogen activated protein kinase-dependent mechanism. **J. Neurochem.** 87 (2003) 1546-1557.

21. Sebok, A., Nusser, N., Debreceni, B., Guo, Z., Santos, M.F., Szeberenyi, J. and Tigyi, G. Different roles for RhoA during neurite initiation, elongation, and regeneration in PC12 cells. **J. Neurochem.** 73 (1999) 949-960.

22. Tojima, T. and Ito, E. Signal transduction cascades underlying de novo protein synthesis required for neuronal morphogenesis in differentiating neurons. **Prog. Neurobiol.** 72 (2004) 183-193.

23. Dent, E.W. and Gertler, F.B. Cytoskeletal dynamics and transport in growth cone motility and axon guidance. **Neuron** 40 (2003) 209-227.

24. Maekawa, M., Ishizaki, T., Boku, S., Watanabe, N., Fujita, A., Iwamatsu, A., Obinata, T., Ohashi, K., Mizuno, K. and Narumiya, S. Signaling from Rho to the actin cytoskeleton through protein kinases ROCK and LIM-kinase. **Science** 285 (1999) 895-898.

25. Ohashi, K., Nagata, K., Maekawa, M., Ishizaki, T., Narumiya, S. and Mizuno, K. Rho-associated kinase ROCK activates LIM-kinase 1 by phosphorylation at threonine 508 within the activation loop. **J. Biol. Chem.** 275 (2000) 3577-3582.

26. Hashimoto, R., Nakamura, Y., Goto, H., Wada, Y., Sakoda, S., Kaibuchi, K., Inagaki, M. and Takeda, M. Domain- and site-specific phosphorylation of bovine NF-L by Rho-associated kinase. **Biochem. Biophys. Res. Commun.** 245 (1998) 407-411.

27. Amano, M., Kaneko, T., Maeda, A., Nakayama, M., Ito, M., Yamauchi, T., Goto, H., Fukata, Y., Oshiro, N., Shinohara, A., Iwamatsu, A. and Kaibuchi,

K. Identification of Tau and MAP2 as novel substrates of Rho-kinase and myosin phosphatase. **J. Neurochem.** 87 (2003) 780-790.

28. Davies, S.P., Reddy, H., Caivano, M. and Cohen, P. Specificity and mechanism of action of some commonly used protein kinase inhibitors. **Biochem. J.** 351 (2000) 95-105.

29. Ikenoya, M., Hidaka, H., Hosoya, T., Suzuki, M., Yamamoto, N. and Sasaki, Y. Inhibition of rho-kinase-induced myristoylated alanine-rich C kinase substrate (MARCKS) phosphorylation in human neuronal cells by H-1152, a novel and specific Rho-kinase inhibitor. **J. Neurochem.** 81 (2002) 9-16.

30. Nakajima, M., Hayashi, K., Egi, Y., Katayama, K., Amano, Y., Uehata, M., Ohtsuki, M., Fujii, A., Oshita, K., Kataoka, H., Chiba, K., Goto, N. and Kondo, T. Effect of Wf-536, a novel ROCK inhibitor, against metastasis of B16 melanoma. **Cancer Chemother. Pharmacol.** 52 (2003) 319-324.

31. Ishizaki, T., Uehata, M., Tamechika, I., Keel, J., Nonomura, K., Maekawa, M. and Narumiya, S. Pharmacological properties of Y-27632, a specific inhibitor of rho-associated kinases. **Mol. Pharmacol.** 57 (2000) 976-983.

32. Christensen, A.E., Selheim, F., de Rooij, J., Dremier, S., Schwede, F., Dao, K.K., Martinez, A., Maenhaut, C., Bos, J.L., Genieser, H.G. and Doskeland, S.O. cAMP analog mapping of Epac1 and cAMP kinase. Discriminating analogs demonstrate that Epac and cAMP kinase act synergistically to promote PC-12 cell neurite extension. **J. Biol. Chem.** 278 (2003) 35394-35402.

33. Hundle, B., McMahon, T., Dadgar, J. and Messing, R.O. Overexpression of epsilon-protein kinase C enhances nerve growth factor-induced phosphorylation of mitogen-activated protein kinases and neurite outgrowth. **J. Biol. Chem.** 270 (1995) 30134-30140.

34. Obara, Y., Aoki, T., Kusano, M. and Ohizumi, Y. Beta-eudesmol induces neurite outgrowth in rat pheochromocytoma cells accompanied by an activation of mitogen-activated protein kinase. **J. Pharmacol. Exp. Ther.** 301 (2002) 803-811.

35. Birkenfeld, J., Betz, H. and Roth, D. Inhibition of neurite extension by overexpression of individual domains of LIM kinase 1. **J. Neurochem.** 78 (2001) 924-927.

36. Fujita, A., Hattori, Y., Takeuchi, T., Kamata, Y. and Hata, F. NGF induces neurite outgrowth via a decrease in phosphorylation of myosin light chain in PC12 cells. **Neuroreport** 12 (2001) 3599-3602.

37. Kishida, S., Yamamoto, H. and Kikuchi, A. Wnt-3a and Dvl induce neurite retraction by activating Rho-associated kinase. **Mol. Cell Biol.** 24 (2004) 4487-4501.

38. Sasaki, Y., Suzuki, M. and Hidaka, H. The novel and specific Rho-kinase inhibitor (S)-(+)-2-methyl-1-[(4-methyl-5-isoquinoline)sulfonyl]-homopiperazine as a probing molecule for Rho-kinase-involved pathway. **Pharmacol. Ther.** 93 (2002) 225-232.

39. Braun, H., Schafer, K. and Hollt, V. BetaIII tubulin-expressing neurons reveal enhanced neurogenesis in hippocampal and cortical structures after a contusion trauma in rats. **J. Neurotrauma** 19 (2002) 975-983.
40. Aizawa, H., Wakatsuki, S., Ishii, A., Moriyama, K., Sasaki, Y., Ohashi, K., Sekine-Aizawa, Y., Sehara-Fujisawa, A., Mizuno, K., Goshima, Y. and Yahara, I. Phosphorylation of cofilin by LIM-kinase is necessary for semaphorin 3A-induced growth cone collapse. **Nat. Neurosci.** 4 (2001) 367-373.
41. Niwa, R., Nagata-Ohashi, K., Takeichi, M., Mizuno, K. and Uemura, T. Control of actin reorganization by Slingshot, a family of phosphatases that dephosphorylate ADF/cofilin. **Cell** 108 (2002) 233-246.
42. Ambach, A., Saunus, J., Konstandin, M., Wesselborg, S., Meuer, S.C. and Samstag, Y. The serine phosphatases PP1 and PP2A associate with and activate the actin-binding protein cofilin in human T lymphocytes. **Eur. J. Immunol.** 30 (2000) 3422-3431.
43. Revenu, C., Athman, R., Robine, S. and Louvard, D. The co-workers of actin filaments: from cell structures to signals. **Nat. Rev. Mol. Cell Biol.** 5 (2004) 635-646.
44. Zhou, Y., Su, Y., Li, B., Liu, F., Ryder, J.W., Wu, X., Gonzalez-DeWhitt, P.A., Gelfanova, V., Hale, J.E., May, P.C., Paul, S.M. and Ni, B. Nonsteroidal anti-inflammatory drugs can lower amyloidogenic Abeta42 by inhibiting Rho. **Science** 302 (2003) 1215-1217.
45. Ellezam, B., Dubreuil, C., Winton, M., Loy, L., Dergham, P., Selles-Navarro, I. and McKerracher, L. Inactivation of intracellular Rho to stimulate axon growth and regeneration. **Prog. Brain. Res.** 137 (2002) 371-380.
46. Brabeck, C., Beschorner, R., Conrad, S., Mittelbronn, M., Bekure, K., Meyermann, R., Schluesener, H.J. and Schwab, J.M. Lesional expression of RhoA and RhoB following traumatic brain injury in humans. **J. Neurotrauma** 21 (2004) 697-706.
47. Brabeck, C., Mittelbronn, M., Bekure, K., Meyermann, R., Schluesener, H.J. and Schwab, J.M. Effect of focal cerebral infarctions on lesional RhoA and RhoB expression. **Arch. Neurol.** 60 (2003) 1245-1249.